Peer-reviewed version available at Electronics 2018, 7, 143; doi:10.3390/electronics7080143

Article

MWCNT-Epoxy Nanocomposite Sensors for Structural Health Monitoring

Omid Sam-Daliri[1,2], Lisa-Marie Faller[2,*], Mohammadreza Farahani[1], Ali Roshanghias[3], Hannes Oberlercher[4], Tobias Mitterer[2], Alireza Araee[1], and Hubert Zangl[2]

[1] School of Mechanical Engineering, College of Engineering, University of Tehran, Tehran, Iran; omid_sam@ut.ac.ir; mrfarahani@ut.ac.ir; alaraee@ut.ac.ir
[2] Institute of Smart Systems Technologies, Alpen-Adria-Universität Klagenfurt, 9020 Klagenfurt, Austria; Omid.Samdaliri@aau.at; Tobias.Mitterer@aau.at; Hubert.Zangl@aau.at
[3] CTR Carinthian Tech Research AG, 9524 Villach, Austria; Ali.Roshanghias@ctr.at
[4] Carinthian University of Applied Sciences, 9524 Villach, Austria; H.Oberlercher@fh-kaernten.at
* Correspondence: Lisa-Marie.Faller@aau.at; Tel.: +43 463 2700 3563

Abstract: We address Multi-Wall Carbon NanoTubes (MWCNTs) for structural health monitoring in adhesive bonds such as in building structures. MWCNT-loaded composites are employed to sense strain changes under tension load using an AC impedance measurement setup. Different weight percentages of 1, 1.5, 2 and 3 wt.% MWCNT are added to the base epoxy resin using different dispersion times, i.e. 5, 10 and 15 minutes. The equivalent parallel resistance of the specimens is measured by applying an alternating voltage at different frequencies. To determine the mechanical as well as sensory properties, the specimens are subjected to a tensile test with concurrent impedance measurement. Using alternating voltage, a higher sensitivity of the impedance reading can be achieved. Employing these sensors in buildings and combining the readings of a network of such devices can significantly improve the buildings' safety. Additionally, networks of such sensors can be used to identify necessary maintenance actions and locations.

Keywords: carbon nanotubes; nanocomposite sensor; tensile testing; impedance measurement

1. Introduction

The aim to fabricate smart composite structures to improve safety and to monitor structures as part of our living environment has resulted in a major research effort regarding the composition and performance of composites employing advanced materials. Advanced materials are used to fabricate smart sensors based on carbon particles such as carbon fibers, carbon blocks, graphite [1,2] and also MWCNTs. MWCNTs have distinctive mechanical and electrical properties. They provide a unique potential to improve the mechanical [3-5] as well as electrical properties [6-10] of polymer-matrix composites. MWCNT- epoxy adhesive are used for applications such as electronic devices, smart adhesive joints in buildings and bus structures [11-13] and gas sensors [14]. In [3] the authors study the tensile behavior of Carbon Nanotubes (CNT)-loaded epoxy nanocomposite films, and report that, by adding CNTs to the polymer matrix, the tensile modulus, yield strength and ultimate strength of the final polymer films can be increased. In [7], the electrical properties of CNT-epoxy nanocomposites were improved by surface treatment of the CNT specimens. A comparison of the electrical and mechanical properties of various carbon-loaded composites with a focus on their piezo-resistive properties is presented in [15].

The changes in the electrical resistance result from deformations and failures within the polymer matrix when the composites are subjected to mechanical loading [16-18]. The two predominant factors governing the resulting resistance are [19]: first, the contact between two adjacent carbon nanotubes which might be broken; second, the change in the tunneling resistance between two

Peer-reviewed version available at Electronics 2018, 7, 143; doi:10.3390/electronics7080143

adjacent carbon nanotubes due to variation of the distance between them. A detailed elaboration of the mechanisms governing the change of the electrical resistance of MWCNT-epoxy nanocomposites under mechanical stress is given in [20]. Based on these changes in electrical resistance, MWCNT thin films have been employed for damage sensing [21-23], and CNT-loaded composites were suggested as strain sensors in the industrial sector for health monitoring [24-26].

It has further been shown that the morphological properties of carbon nanoparticles influence the response of the respective nanocomposite sensors [27]. The nanocomposite sensors are comprised of conductive networks or agglomerates distributed within the polymer matrix where MWCNT form 1D structures. The network conductivity is further affected by the weight percentage of the nanoparticles, mutual interactions between them and their state of dispersion in the polymer matrix [28,29] which strongly depend on the preparation and activation process.

In this work, we present a study which investigates the influence of weight percentage of MWCNT and its dispersion time on the Alternating Current (AC) impedance. This AC impedance measurement can provide higher sensitivity by considering also the electrostatic properties of the material. Considering also such frequency dependent parameters, the sensing functionality of MWCNT-epoxy composites can thus be exploiting or even improved investing less energy. This presents a novelty compared to aforementioned studies, where Direct Current (DC) measurement is employed to determine the electrical properties of the considered specimens.

Low necessary energy facilitates the design of autarkic sensor systems [30] to monitor building structures. Using technologies such as Transducer Electronic DataSheets (TEDS) [31] these devices can additionally be integrated into modern building automation facilities. There, a network of such sensors can provide information on the health state of a building and indicate necessary maintenance.

In Sec. 2 the material and equipment needed for the preparation method, as well as the mechanical and electrical testing of the nanocomposites is presented. First, the preparation method, which consists of only basic steps such as mixing and deagglomeration is introduced. Then, the tensile testing machine and the electrical impedance measurement for, first the percolation threshold, and secondly during the tensile testing are described. In Sec. 3 the results for the percolation threshold measurements and tensile testing are described, then the microstructure of the nanocomposites is presented based on Scanning Electron Microscopy (SEM) images. Finally, in Sec. 4 concluding remarks on the presented study are given.

2. Materials and Methods

2.1. Materials

The base of the prepared nanocomposites is epoxy as matrix and MWCNTs as the conductive nanofiller. The used epoxy resin is EpoThin® (Buehler, Germany), a free flowing, low viscosity, low shrinkage epoxy resin which allows the nanofiller to easily distribute in the EpoThin matrix. It has a typical cure time of nine hours at 27°C. MWCNTs as the conductive nanoparticles by Cheaptube (USA) were used. The outer diameter of the considered MWCNT is 30 to 50 nm. The length of the used MWCNT is between 10 to 20 μm with a purity more than 95%.

2.2. Preparation of Specimens

Due to the exploitation of the conduction as well as electrostatic effect occurring in the specimen, the fabrication process can be kept less sophisticated than those reported in previous work [32,33] without significant loss of sensory properties.

Weighed amounts of epoxy resin and carbon nanotubes (measured by a digital scale with accuracy equal to 0.1 mg) were mechanically stirred for 5 min in a beaker. The mixture was then placed in a shear mixer (IKA T18 digital ULTRA TURRAX), at 1000 RPM for 15 min. Then, the dispersion of the MWCNT in the epoxy resin was further accomplished using an ultrasonic bath (see Figure 1 (a)). Effective means of deagglomerating and dispersing are needed to overcome the bonding forces after wettening the powders. Therefore, ultrasonic bath with high frequency (35-60 kHz) was used to disperse the MWCNT in the epoxy resin appropriately and break agglomerated particles. The

Peer-reviewed version available at Electronics 2018, 7, 143; doi:10.3390/electronics7080143

time was set according to the considered respective time of dispersion (see Tab.1) and the environmental temperature was kept constant at 25oC. Thus, CNTs with weight percentages of 1, 1.5, 2 and 3 wt.% were dispersed in the epoxy matrix at different dispersion times. The resin was then combined with hardener in the ratio of 2:1 for 15 min on the stirrer and was immediately poured into the dog-bone molds. After 24 hours, the dog-bone shape samples for tensile testing were extracted from the mold. The mold was designed according to the ASTM D638 standard. In this process, we avoid commonly employed, often complex, activation procedures.

Table 1. Processing conditions of CNT-epoxy sensor

Amount of CNT	Dispersion time
1; 1.5; 2, 3	5; 10; 15

To facilitate the electrical measurement of the samples, two metallic wires were applied close to the necking end parts at a specific distance of 7.5 cm. The wires are fixed using conductive silver adhesive. The surface-ring contact was used to minimize electrical contact resistance (see Fig. 1 (b)).

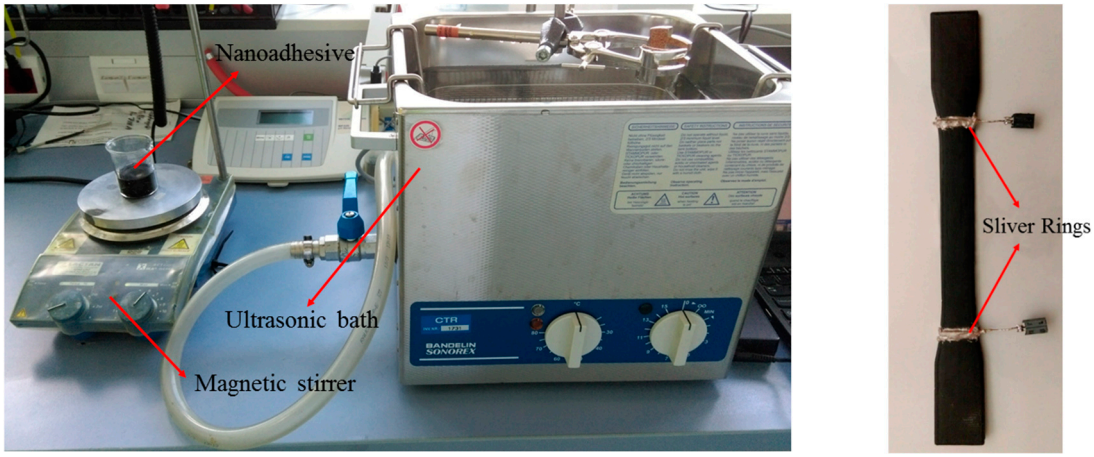

(**a**) (**b**)

Figure. 1. (a) Magnetic stirrer and ultrasonic bath (b) nanocomposite specimen

2.3. Mechanical and Electrical Acquisition System

Three specimens were prepared under equivalent conditions for each test case of this study, and the effect of the dispersion time and various filler contents were investigated on the initial equivalent parallel resistance. Then, the specimens were subjected to a longitudinal loading until fracture using a Zwick/Roell Z020 universal testing machine (see Figure 2). The crosshead displacement rate of 1 mm/min was applied according to the standard for polymer testing. The tensile force, longitudinal displacement and voltage changes were measured simultaneously versus time.

Electrical measurements were conducted in two steps. The first step was to determine the frequency dependent initial equivalent parallel resistance of the specimens using an LCR measurement bridge by Extech Instruments. This instrument determines the equivalent parallel resistance at different frequency settings. The shape of the resulting measurement curves can be analysed to determine the respective percolation threshold of the samples: for non-conducting materials, the resistance will decrease with increasing frequency. This is due to the predominant capacitive effect that can be observed here. Above the percolation threshold, the resistive behavior will dominate and the impedance of the samples stays constant over frequency.

The second step is the impedance measurement during the tensile test. These measurements are done using a high-speed, high-resolution measurement platform [34,35]. It is based on an FPGA-system with a customized analog front-end to enable high-speed, high-resolution measurements. For

series production, the components can be integrated into a system which in size and costs is well suitable for the application of commercial structural health monitoring in buildings.

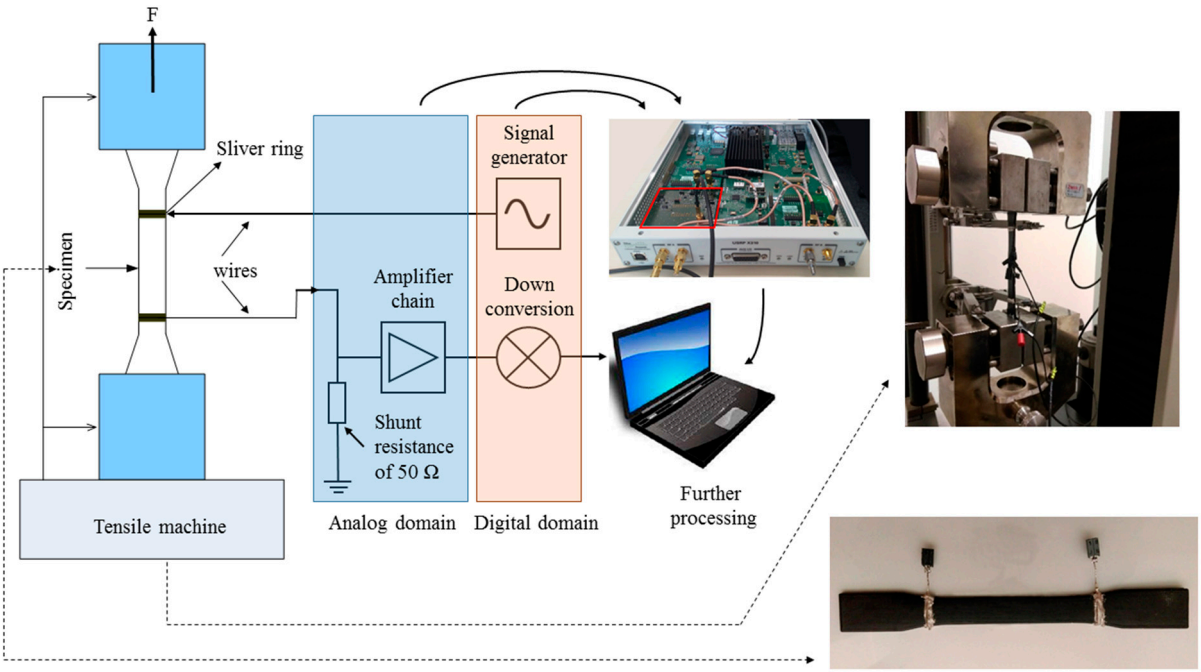

Figure 2. Illustration of the impedance measurement setup during the tensile test. The arrows indicate that the analog hardware as well as the digital domain signal processing are part of the used measurement platform.

The measurement setup is also illustrated in Fig 2.: Left is the nanocomposite specimen which, on one side, is connected to the input analog amplifier chain as part of the impedance measurement hardware. The other side is connected to the output which supplies a digitally generated sine signal. In the digital domain, the measurement platform also supplies the algorithms necessary for signal processing, e.g. down-conversion of the acquired signal. Down-conversion is done, to transfer the measurement signal from a higher measurement frequency to a lower frequency together with a reduction of the necessary number of samples. The results can then be used for further processing for, e.g. analysis and visualization.

A higher measurement frequency can, in the first place, be beneficial to avoid or reduce the influence of other electrical equipment present near the sensors. This is important when these nanocomposite sensors are to be employed in buildings which commonly suffer from high electric emissions due to the used machinery and other equipment. Even novel washing machines produce massive electrical emissions. Secondly, in this application, we assume to achieve improved impedance readings also for samples below the percolation threshold through the application of a high frequency measurement signal. Thus, also samples with less attractive electrical properties, but prepared using a simplified less time-consuming fabrication process might as well be used for sensing.

Through preliminary analysis, the measurements frequency was chosen to be 100 kHz with an excitation voltage of 1 V (signal generator in Figure 2). Via the shunt resistance of 50 Ω (see Figure 2), a voltage reading is recorded which is proportional to the resistance of the sample. For a resistance change, the voltage signal also changes accordingly. To determine the impedance as illustrated in the following diagrams, first a calibration measurement using a known resistance is done. Using this calibration measurement, and a proportionality factor (to correct for the shunt resistance), the recorded voltage reading can be corrected to give the equivalent impedance.

3. Results and Discussions

3.1. Achieved Impedance Without Mechanical Loading

The equivalent parallel resistance of the nanocomposite specimens changes significantly when measured at different frequencies. The results of this initial resistance measurements are illustrated for dispersion times of 10 and 15 minutes in Fig.s 3 and 4, respectively. In all of these diagrams, the equivalent parallel resistance decreases with increasing frequency. It can be seen from the Figure 3 that, when the filler content of MWCNT increased up to 3 wt.%, the resistance decreases from 180 MΩ to less than 6 MΩ given the same dispersion time. The equivalent parallel resistance clearly shows a flat curve shape at 3 wt.%. At this point, the transition from insulating to the conductive phase, called percolation threshold, is observed. The experimental method for the determination of the respective percolation threshold measurement was in compliance with the method used in [36]. Due to simplifications in the preparation process of the samples, the percolation threshold was achieved with samples containing higher weight percent of CNT.

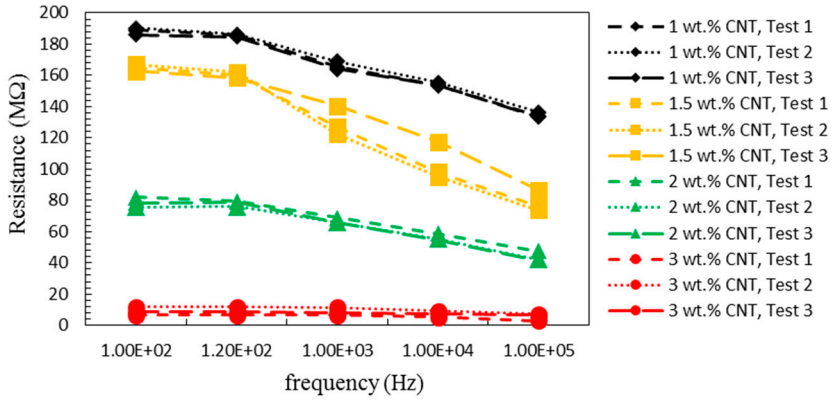

Figure 3. Equivalent parallel resistance of nanocomposite sensor with MWCNT filler content for dispersion time equal to 10 min.

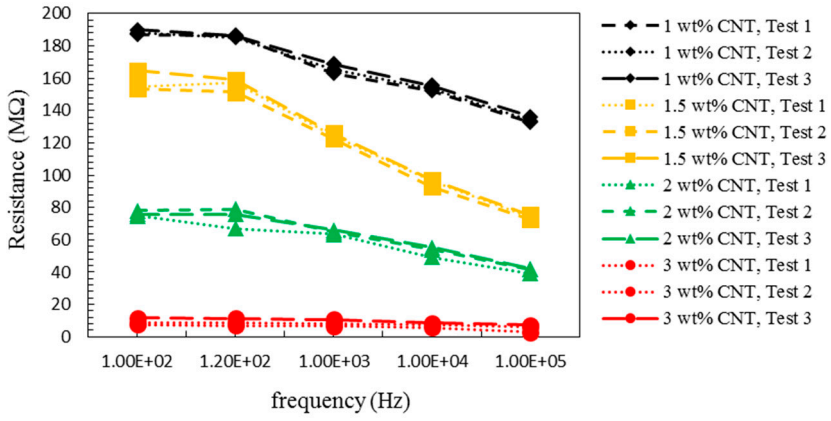

Figure 4. Equivalent parallel resistance of nanocomposite sensor with MWCNT filler content for dispersion time equal to 15 min.

Conductive networks are formed in the epoxy matrix as conductive fillers are distributed appropriately within the epoxy matrix by good dispersion [37]. As a result, the initial resistance changes with the employed dispersion time.

Based on the equivalent parallel resistance value, the effect of dispersion time was investigated using statistical analysis by Minitab software (see Figure 5 (a) and (b)). Since the resistance does not change significantly for an increase of the dispersion time above 10 min, this value could be identified

as sufficient with respect to the given process settings. Additionally, this analysis shows that the effect of the dispersion time is higher at low weight percent of MWCNT.

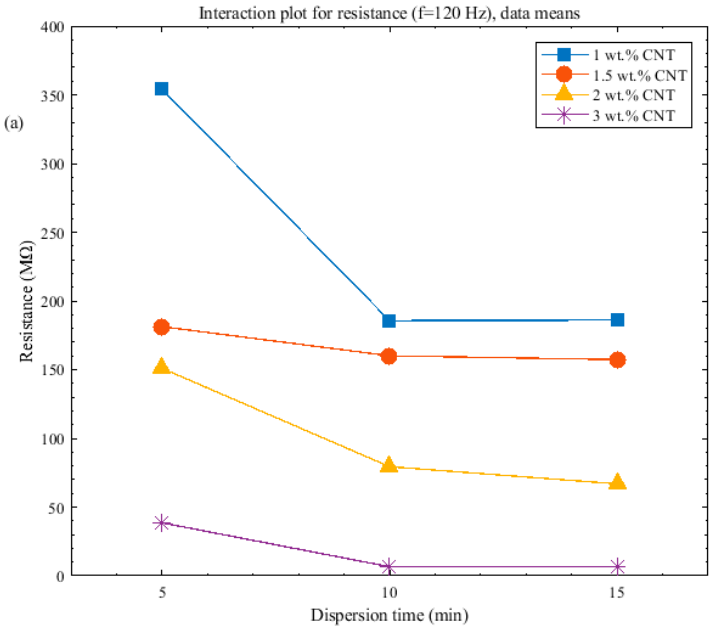

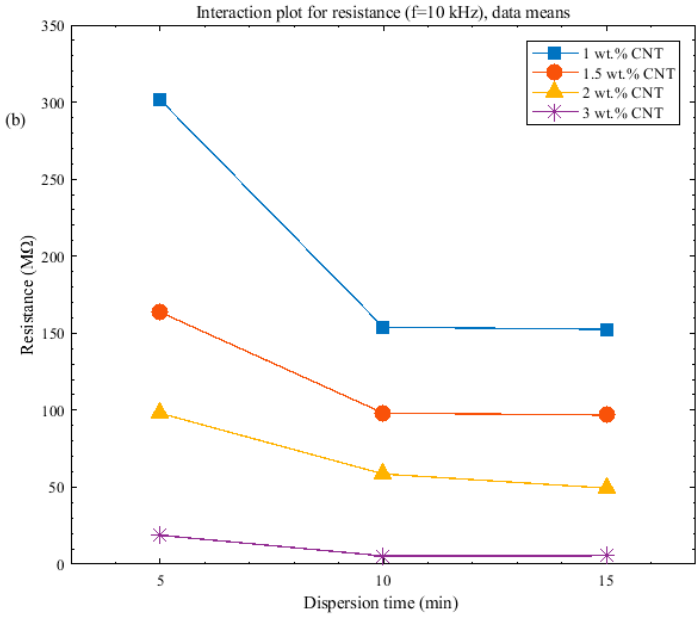

Figure 5. Interaction plot of the weight percent and dispersion time for resistance in different frequencies (a) 120 Hz (b) 10 kHz.

3.2. Morphology

The dispersion of MWCNT in the epoxy resin was validated using SEM images. SEM pictures of the fracture surface of the nanocomposite specimen were taken after the tensile test. In Fig. 6 (a) and (b) SEM images of nanocomposites containing 2 wt.% MWCNT at lower and higher magnifications in 5 min dispersion time are given. The highlighted circles in Fig. 6 (a) and (b) mark agglomerated zones of MWCNT in the epoxy matrix. When compared to the scale given at the lower right corner of the images, it can be seen that the size of the highlighted zones is between 10 and 20 μm (see Fig. 6 (b)). Although, high degrees of agglomeration have to be avoided when preparing MWCNT-composites, agglomeration zones of diameters larger than 10 μm are required to achieve

sufficient conductivity. Additionally, we observed a nearly uniform distribution of MWCNTs in the epoxy matrix with increasing dispersion time and weight percent (see Figure 6 (c)). These observations now qualify the suggested simplified process as suitable for the fabrication of nanocomposites with proper sensory functionality.

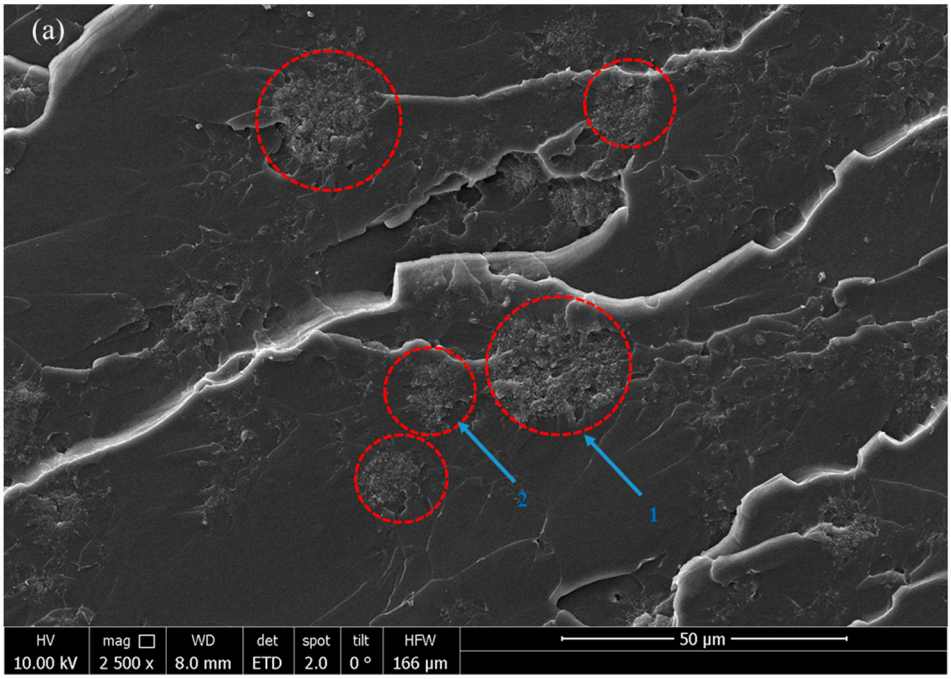

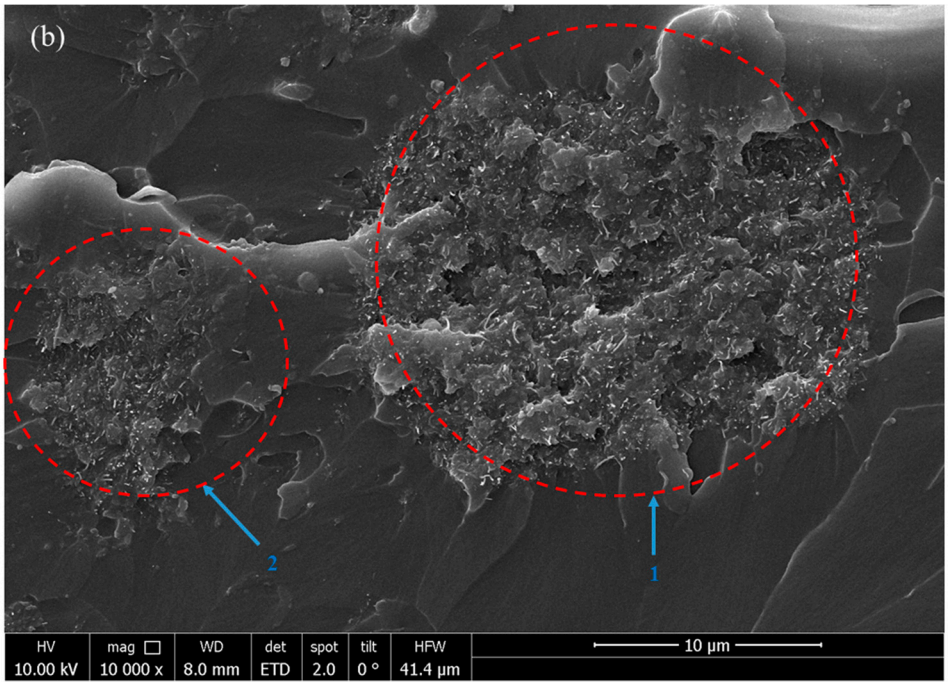

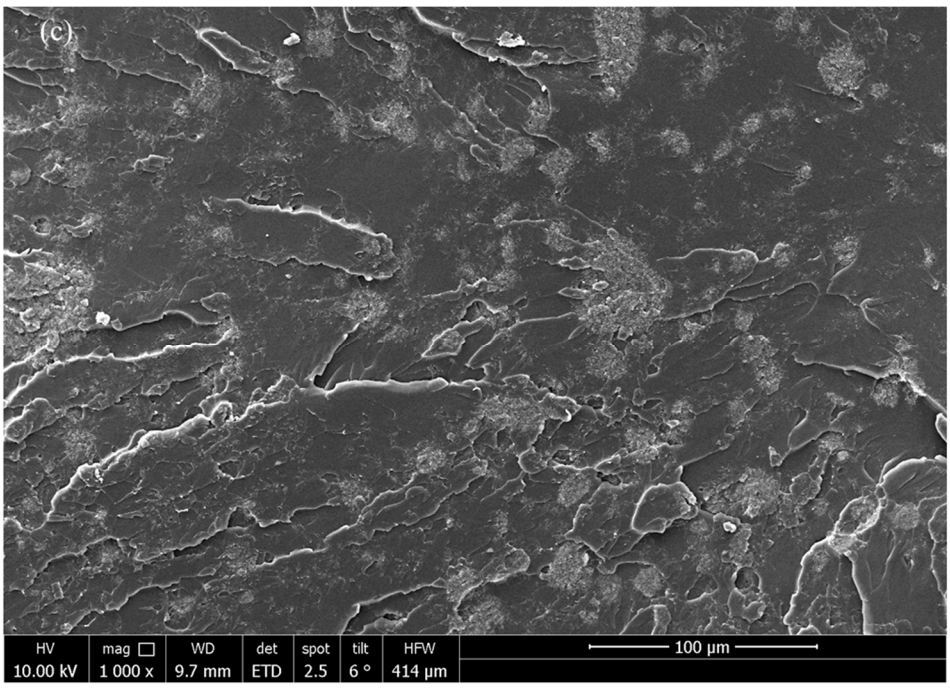

Figure 6. Fracture surface images of MWCNT- epoxy nanocomposite with (a) 2 wt.% MWCNT with magnification of 2500x at 5 min dispersion time and (b) 2 wt.% MWCNT with magnification of 10000x at 5 min dispersion time, and (c) 3 wt.% MWCNT at 10 min dispersion time.

3.3. Sensing Capabilities During Mechanical Loading

The majority of previous studies used the two-probe method to measure the electrical resistance changes during the tensile test [38-40], which may provide disadvantages for the DC measurements. Here we use an AC measurement setup at an intermediate frequency, therefore the two probe method is sufficient and the cumbersome preparation of two additional connections per specimen can be avoided. In the following Fig.s we report the absolute impedance change value in contrast to other research which focuses on piezoelectric effects and thus reports a relative resistance change $\Delta R/R$, thus the graphs presented here exhibit different shapes. According to the diagrams in Fig. 8, for specimens with a filler content of 2 wt. % MWCNT and the lowest dispersion time of 5 min., a non-convex curve for the electrical resistance measurement was observed (see Fig. 7 (a)). The steep curve segments result from deferments of large agglomeration zones of CNTs in the epoxy matrix present due to the low dispersion time. The shape of the electrical resistance changes curves improved for a dispersion time of 10 and 15 min. as depicted in Fig.s 7 (b) and (c). The curve observed for 3 wt.% MWCNT is nearly convex and thus qualifies the fabricated nanocomposites for continuous sensing of damage and damage progression. Fig. 8 shows the resistance change for a nanocomposite specimen including 3 wt. % MWCNT with a dispersion time value of 5 min. Nanocomposite specimens with higher percentage of carbon nanotubes generally exhibit a steeper slope in the electrical resistance change (see Figure 9). This result is consistent with the SEM image of the nanocomposite obtained at 3 wt.% MWCNT with 10 min dispersion time (see Figure 6 (c)) which displayed a nearly uniform distribution. This filler amount was equal to the percolation threshold value obtained from AC measurement using the LCR meter. In comparison to the specimens including 1 and 2 wt.% MWCNT, the slope of the resistance changes diagram for the specimens with 3 wt. % MWCNT also exhibits a smoother shape. Georgousiset al. [36] reported that the highest sensitivity can be achieved close to the percolation threshold. In the present study, we confirm these result showing that the smoothest curves are achieved above the persolation threshold. Obviously, the samples below the percolation threshold (1, 1.5 and 2 wt. %) can be used for sensing by applying an AC impedance measurement setup and a suitable calibration method to correct for the non-smooth curve shape.

Based on the max. forces of the specimens using different dispersion time, the max. strength was obtained for every weight percent (Tab. 2), a significant difference could be observed between the maximum forces achieved for specimens containing different percentages of MWCNT. The specimens including 3 wt.% MWCNT could withstand less longitudinal force. It can further be seen from Tab. 2 that increasing the filler amount from 1 to 3 wt.%, the maximum strength decreases from 68.36 MPa to 50.19 MPa. In general, the strength of nanocomposites obtained from tensile tests were improved by adding MWCNT to the epoxy matrix. As reported in Tab. 2, the maximum strength of the nanocomposites increased with respect to pure epoxy. However, the maximum strength decreased by adding more than 1 wt.% MWCNT similar as reported in [41].

The slopes of the electrical impedance diagrams show that a filler amount equal to 3 wt.% CNT provides the best damage sensing properties. However, the mechanical strength decreased to 50.19 MPa.

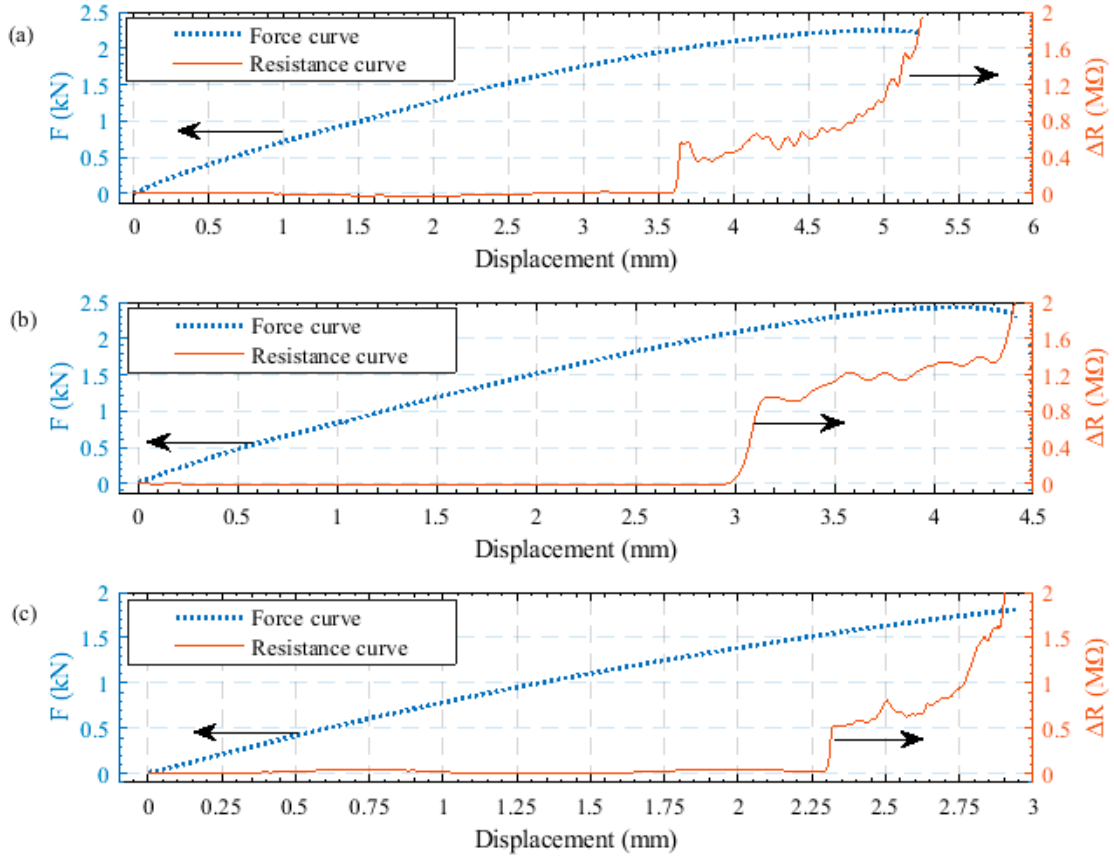

Figure 7. Load- displacement and resistance curves for the nanocomposite sensor with 2 wt.% MWCNT for different dispersion time (a) 5 minutes, (b) 10 minutes and (c) 15 min. The arrows indicate the axis belonging to the respective curve.

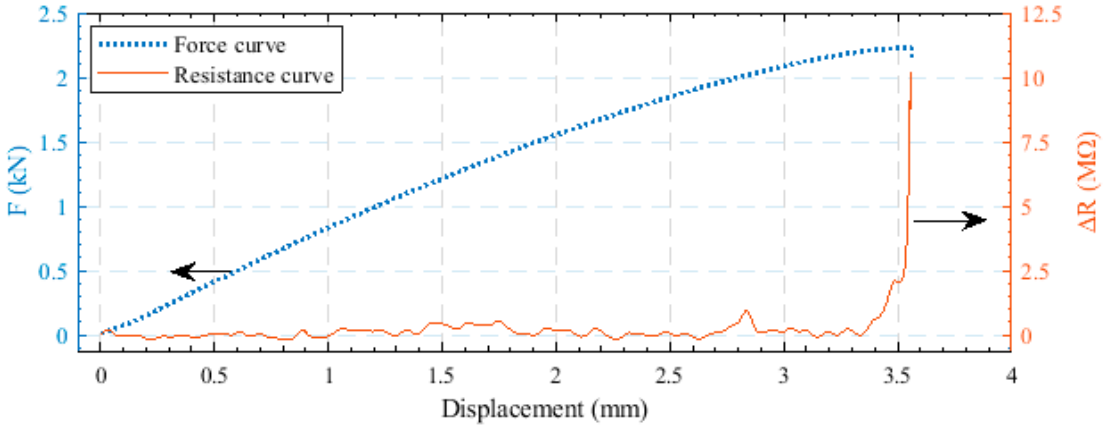

Figure 8. Load-displacement and resistance curves for the nanocomposite sensor with 3 wt.% MWCNT at 5 minutes

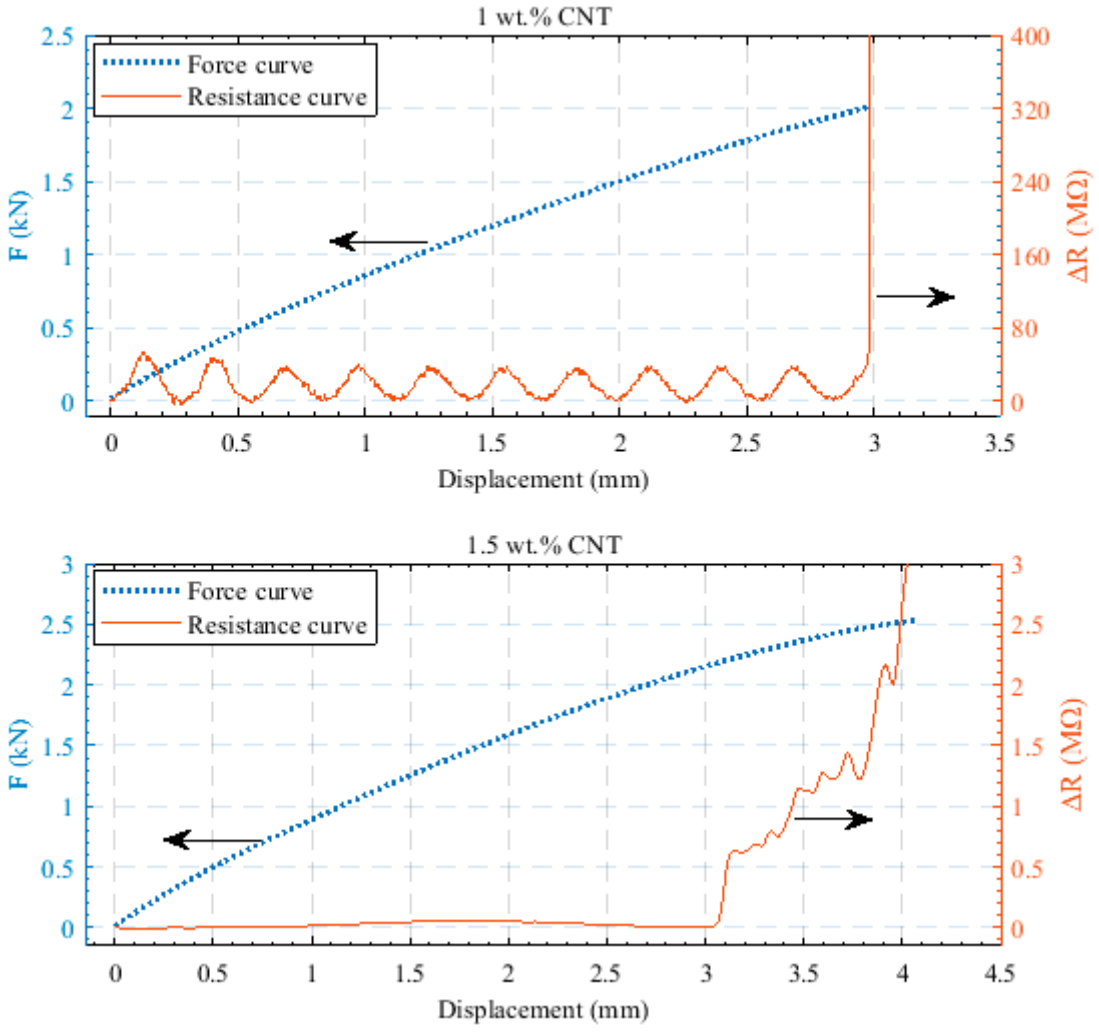

Preprints (www.preprints.org) | NOT PEER-REVIEWED | Posted: 23 July 2018 doi:10.20944/preprints201807.0419.v1

Peer-reviewed version available at Electronics 2018, 7, 143; doi:10.3390/electronics7080143

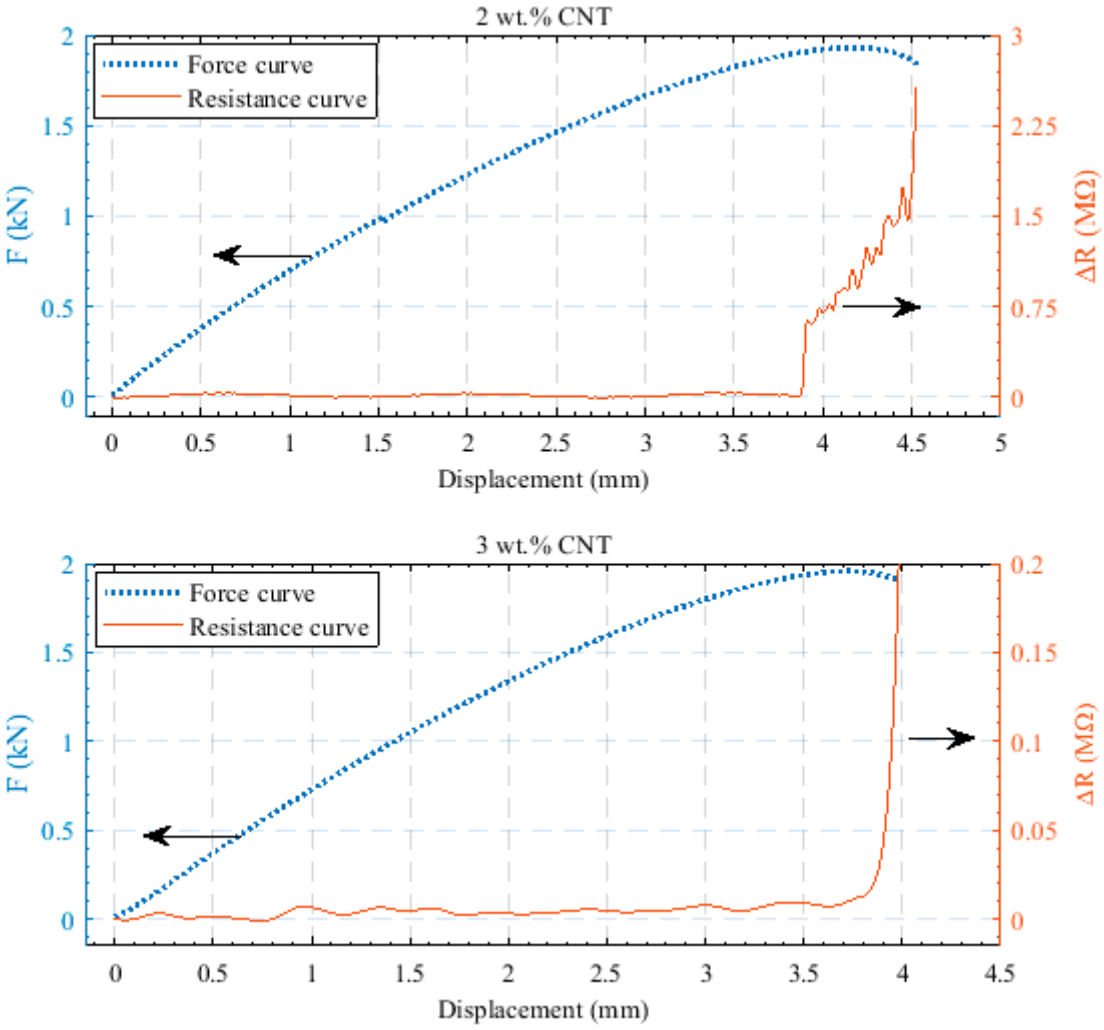

Figure 9. Force and resistance changes as a function of displacement for nanocomposites with different weight percent prepared at 10 min dispersion time.

Table 2. Mechanical properties of the nanocomposites.

Specimen	Young's modulus (GPa)	Max. strength (MPa)
Pure epoxy	3.533	47.19
1 wt. % CNT-epoxy	3.045	68.36
1.5 wt. % CNT-epoxy	3.109	64.89
2 wt. % CNT-epoxy	2.932	62.26
3 wt. % CNT-epoxy	2.008	50.19

4. Conclusion

In this work, we introduce a measurement technique for condition monitoring of damage in single adhesive joints for structures and buildings by conductive nanoadhesive. The conductive nanoadhesive was prepared with various MWCNT contents and different dispersion times. Then,

the capability of the prepared MWCNT-epoxy composites as nanocomposite sensors was studied by determining their electrical impedance changes during longitudinal loading. It was observed that dispersion times longer than 10 min provide no significant improvement in the equivalent parallel resistance of the nanocomposite. Although the maximum tolerated forces of these nanocomposite sensors were achieved with 1 wt.% MWCNT content, the nanocomposite sensors fabricated with 3 wt.% MWCNT and a dispersion time of 10 minutes showed better self-damage sensing capabilities while still achieving a mechanical strength higher than that of pure epoxy.

Acknowledgement

This study was financially supported by the Alpen-Adria-Universität. The preparation of specimens was conducted in the chemistry lab of the Carinthian Tech Research (CTR) AG and mechanical testing equipment was supplied by the Carinthian University of Applied Sciences (FH Kärnten) in Villach.

References

1. Lu, J.; Chen, X.; Lu, W.; Chen, G. The piezoresistive behaviors of polyethylene/foliated graphite nanocomposites. *European Polymer Journal* **2006**, *42*, 1015-1021.
2. Le, J.-L.; Du, H.; Dai Pang, S. Use of 2d graphene nanoplatelets (gnp) in cement composites for structural health evaluation. *Composites Part B: Engineering* **2014**, *67*, 555-563.
3. Thostenson, E.T.; Chou, T.-W. Aligned multi-walled carbon nanotube-reinforced composites: Processing and mechanical characterization. *Journal of Physics D: Applied Physics* **2002**, *35*, L77.
4. Suhr, J.; Koratkar, N.; Keblinski, P.; Ajayan, P. Viscoelasticity in carbon nanotube composites. *Nature Materials* **2005**, *4*, 134.
5. Cha, J.; Jun, G.H.; Park, J.K.; Kim, J.C.; Ryu, H.J.; Hong, S.H. Improvement of modulus, strength and fracture toughness of cnt/epoxy nanocomposites through the functionalization of carbon nanotubes. *Composites Part B: Engineering* **2017**, *129*, 169-179.
6. Wang, L.; Dang, Z.-M. Carbon nanotube composites with high dielectric constant at low percolation threshold. *Applied Physics Letters* **2005**, *87*, 042903.
7. Li, J.; Zhang, G.; Zhang, H.; Fan, X.; Zhou, L.; Shang, Z.; Shi, X. Electrical conductivity and electromagnetic interference shielding of epoxy nanocomposite foams containing functionalized multi-wall carbon nanotubes. *Applied Surface Science* **2018**, *428*, 7-16.
8. Guadagno, L.; Raimondo, M.; Vertuccio, L.; Naddeo, C.; Barra, G.; Longo, P.; Lamberti, P.; Spinelli, G.; Nobile, M. Morphological, rheological and electrical properties of composites filled with carbon nanotubes functionalized with 1-pyrenebutyric acid. *Composites Part B: Engineering* **2018**.
9. Gardea, F.; Lagoudas, D.C. Characterization of electrical and thermal properties of carbon nanotube/epoxy composites. *Composites Part B: Engineering* **2014**, *56*, 611-620.
10. Krainoi, A.; Kummerlöwe, C.; Nakaramontri, Y.; Vennemann, N.; Pichaiyut, S.; Wisunthorn, S.; Nakason, C. Influence of critical carbon nanotube loading on mechanical and electrical properties of epoxidized natural rubber nanocomposites. *Polymer Testing* **2018**, *66*, 122-136.
11. Galvez, P.; Quesada, A.; Martinez, M.A.; Abenojar, J.; Boada, M.J.L.; Diaz, V. Study of the behaviour of adhesive joints of steel with cfrp for its application in bus structures. *Composites Part B: Engineering* **2017**, *129*, 41-46.
12. Vajtai, R.; Wei, B.; Zhang, Z.; Jung, Y.; Ramanath, G.; Ajayan, P. Building carbon nanotubes and their smart architectures. *Smart Materials and Structures* **2002**, *11*, 691.
13. Koo, Y.; Shanov, V.N.; Yun, Y. Carbon nanotube paper-based electroanalytical devices. *Micromachines* **2016**, *7*, 72.
14. Lee, J.; Lim, S.-H. CNT foam-embedded micro gas pre-concentrator for low-concentration ethane measurements. *Sensors* **2018**, *18*, 1547.
15. Avilés, F.; May-Pat, A.; López-Manchado, M.; Verdejo, R.; Bachmatiuk, A.; Rümmeli, M. A comparative study on the mechanical, electrical and piezoresistive properties of polymer composites using carbon nanostructures of different topology. *European Polymer Journal* **2017**.
16. Nofar, M.; Hoa, S.; Pugh, M. Failure detection and monitoring in polymer matrix composites subjected to static and dynamic loads using carbon nanotube networks. *Composites Science and Technology* **2009**, *69*, 1599-1606.

17. Wang, Y.; Wang, S.; Li, M.; Gu, Y.; Zhang, Z. Piezoresistive response of carbon nanotube composite film under laterally compressive strain. *Sensors and Actuators A: Physical* **2018**.
18. Kim, H.; Kim, Y. High performance flexible piezoelectric pressure sensor based on cnts-doped 0–3 ceramic-epoxy nanocomposites. *Materials & Design* **2018**, *151*, 133-140.
19. Hu, N.; Fukunaga, H.; Atobe, S.; Liu, Y.; Li, J. Piezoresistive strain sensors made from carbon nanotubes based polymer nanocomposites. *Sensors* **2011**, *11*, 10691-10723.
20. Prudencio, E.; Bauman, P.; Williams, S.; Faghihi, D.; Ravi-Chandar, K.; Oden, J. Real-time inference of stochastic damage in composite materials. *Composites Part B: Engineering* **2014**, *67*, 209-219.
21. Kwon, D.-J.; Wang, Z.-J.; Choi, J.-Y.; Shin, P.-S.; DeVries, K.L.; Park, J.-M. Damage sensing and fracture detection of cnt paste using electrical resistance measurements. *Composites Part B: Engineering* **2016**, *90*, 386-391.
22. Mishra, S.; Kumaran, K.; Sivakumaran, R.; Pandian, S.P.; Kundu, S. Synthesis of PVDF/CNT and their functionalized composites for studying their electrical properties to analyze their applicability in actuation & sensing. *Colloids and Surfaces A: Physicochemical and Engineering Aspects* **2016**, *509*, 684-696.
23. Na, W.-J.; Byun, J.-H.; Lee, M.-G.; Yu, W.-R. In-situ damage sensing of woven composites using carbon nanotube conductive networks. *Composites Part A: Applied Science and Manufacturing* **2015**, *77*, 229-236.
24. Li, C.; Thostenson, E.T.; Chou, T.-W. Sensors and actuators based on carbon nanotubes and their composites: A review. *Composites Science and Technology* **2008**, *68*, 1227-1249.
25. Lee, B.M.; Gupta, S.; Loh, K.J.; Nagarajaiah, S. Strain sensing and structural health monitoring using nanofilms and nanocomposites. In *Innovative Developments of Advanced Multifunctional Nanocomposites in Civil and Structural Engineering*, Elsevier: 2016; pp 303-326.
26. Kang, I.; Schulz, M.J.; Kim, J.H.; Shanov, V.; Shi, D. A carbon nanotube strain sensor for structural health monitoring. *Smart Materials and Structures* **2006**, *15*, 737.
27. Meeuw, H.; Viets, C.; Liebig, W.; Schulte, K.; Fiedler, B. Morphological influence of carbon nanofillers on the piezoresistive response of carbon nanoparticle/epoxy composites under mechanical load. *European Polymer Journal* **2016**, *85*, 198-210.
28. Alig, I.; Pötschke, P.; Lellinger, D.; Skipa, T.; Pegel, S.; Kasaliwal, G.R.; Villmow, T. Establishment, morphology and properties of carbon nanotube networks in polymer melts. *Polymer* **2012**, *53*, 4-28.
29. Pal, G.; Kumar, S. Multiscale modeling of effective electrical conductivity of short carbon fiber-carbon nanotube-polymer matrix hybrid composites. *Materials & Design* **2016**, *89*, 129-136.
30. Seyhan, A.T.; Tanoğlu, M.; Schulte, K. Tensile mechanical behavior and fracture toughness of MWCNT and DWCNT modified vinyl-ester/polyester hybrid nanocomposites produced by 3-roll milling. *Materials Science and Engineering: A* **2009**, *523*, 85-92.
31. Kueseng, P.; Sae-oui, P.; Rattanasom, N. Mechanical and electrical properties of natural rubber and nitrile rubber blends filled with multi-wall carbon nanotube: Effect of preparation methods. *Polymer Testing* **2013**, *32*, 731-738.
32. Faller, L.-M.; Mitterer, T.; Leitzke, J.P.; Zangl, H. Design and evaluation of a fast, high-resolution sensor evaluation platform applied to mems position sensing. *IEEE Transactions on Instrumentation and Measurement* **2017**.
33. Faller, L.-M.; Leitzke, J.; Zangl, H. In *Design of a fast, high-resolution sensor evaluation platform applied to a capacitive position sensor for a micromirror*, Instrumentation and Measurement Technology Conference (I2MTC), 2017 IEEE International, 2017; IEEE: pp 1-6.
34. Georgousis, G.; Pandis, C.; Kalamiotis, A.; Georgiopoulos, P.; Kyritsis, A.; Kontou, E.; Pissis, P.; Micusik, M.; Czanikova, K.; Kulicek, J. Strain sensing in polymer/carbon nanotube composites by electrical resistance measurement. *Composites Part B: Engineering* **2015**, *68*, 162-169.
35. Pircheraghi, G.; Powell, T.; Solouki Bonab, V.; Manas-Zloczower, I. Effect of carbon nanotube dispersion and network formation on thermal conductivity of thermoplastic polyurethane/carbon nanotube nanocomposites. *Polymer Engineering & Science* **2016**, *56*, 394-407.
36. Ferrreira, A.; Rocha, J.; Ansón-Casaos, A.; Martínez, M.; Vaz, F.; Lanceros-Mendez, S. Electromechanical performance of poly (vinylidene fluoride)/carbon nanotube composites for strain sensor applications. *Sensors and Actuators A: physical* **2012**, *178*, 10-16.
37. Ku-Herrera, J.; Aviles, F. Cyclic tension and compression piezoresistivity of carbon nanotube/vinyl ester composites in the elastic and plastic regimes. *Carbon* **2012**, *50*, 2592-2598.

38. Grammatikos, S.; Paipetis, A. On the electrical properties of multi scale reinforced composites for damage accumulation monitoring. *Composites Part B: Engineering* **2012**, *43*, 2687-2696.
39. Yu, S.; Tong, M.N.; Critchlow, G. Wedge test of carbon-nanotube-reinforced epoxy adhesive joints. *Journal of Applied Polymer Science* **2009**, *111*, 2957-2962.